Journal of Electroceramics, 13, 321–326, 2004
© 2004 Kluwer Academic Publishers. Manufactured in The Netherlands.

Characterization of Crystalline Carbon Nitride Films Deposited on Si and Si_3N_4/Si Substrate by RF Magnetron Sputtering System with DC Bias

J.G. LEE* & S.P. LEE

Department of Electrical and Electronic Engineering, Kyungnam University, South Korea

Submitted March 2, 2003; Revised March 11, 2004; Accepted May 17, 2004

Abstract. Crystalline carbon nitride films were deposited on Si and Si_3N_4/Si substrate by reactive RF magnetron sputtering system with chamber heating and DC bias. The deposited films showed α-C_3N_4, β-C_3N_4 and lonsdaleite phase by XRD, XPS and FTIR. The crystalline morphology was found to gave a hexagonal structure, which has theoretical unit cell of carbon nitride observed in SEM photographs. When nitrogen gas ratio is 70%, RF power is 300 W and DC bias is –80 V, the growth rate of carbon nitride film on Si_3N_4 substrate is 2.2 μm/hr, which is a relatively high growth rate compared with those in previously reported papers. The deposited films have thermally stable properties in the range of 650°C to 1,400°C.

Keywords: carbon nitride, RF magnetron sputter, crystalline morphology, growth rate

1. Introduction

Cohen and his coworker predicted that a carbon nitride, β-C_3N_4, with a structure similar to that of β-Si_3N_4, may possess extremely high hardness comparable to or harder than that of diamond [1–3]. If crystalline carbon nitride can be formed perfectly, it may have high bulk modulus, low compressibility, high thermal conductivity, high sound velocity [2, 4], high band gap energy, and high electrical resistance [4, 5].

During the last decade, intensive experimental works have been performed to synthesize the theoretically predicted material, β-C_3N_4. Several attempts have been made to synthesize crystalline carbon nitride films by employing sputtering [6, 7], chemical vapor deposition [8, 9], laser ablation [10, 11], and ion beam deposition [12]. Despite the many efforts to synthesize it, the obtained films were amorphous CN_x or very small amount of crystals [13–15]. Furthermore, in the most cases the grown films were seriously nitrogen deficient compared with a stoichiometric β-C_3N_4 (about 57% nitrogen).

We report on the characterization of reactive sputtered carbon nitride films formed under various deposition conditions, such as the substrate type, DC bias, chamber temperature, RF power, and nitrogen ratio. The films were characterized by scanning electron microscopy (SEM), fourier transform infrared (FTIR) spectroscopy, X-ray diffractometer (XRD), X-ray photoelectron spectroscopy(XPS), scanning probe microscopy (SPM) with atomic force microscopy (AFM) and thermogravimetric analyzer & differential temperature analyzer (TGA/DTA).

2. Experimental

The carbon nitride films were deposited on the polished p-type (100) silicon, and on the silicon nitride grown on silicon wafer by reactive RF magnetron sputtering method. The RF power at 13.56 MHz was matched into the capacitive target and plasma via a matching network. A negative DC bias was applied to the substrate module. The schematic diagram of the sputtering system used is shown in Fig. 1. The sputtering target was a high purity (99.999%) graphite. It was mounted on the cathode at a distance between 6 to 10 cm from the

*To whom all correspondence should be addressed. E-mail: ariel98@mail.kyungnam.ac.kr

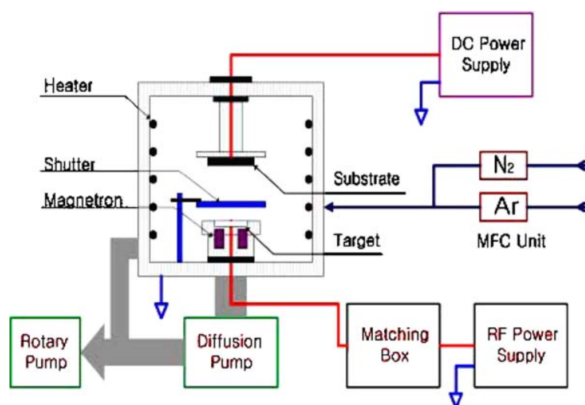

Fig. 1. The schematic diagram of RF reactive magnetron sputtering system.

substrate. The target was pre-sputtered for 20 min prior to each deposition to remove surface contamination. Then the nitrogen (99.999%) gas and Ar (99.999%) gas were introduced into the sputtering chamber through a mass-flow controller (MFC) until the required pressure, 10^{-3}–10^{-2} torr, was obtained. The nitrogen contents of the deposited films were varied by controlling the nitrogen partial pressure in the sputtering gas. To avoid the hydrogen contamination from water molecules on the chamber wall, the chamber was heated to 150°C with the resistively-heated coil. SEM (ABT-32, TOPCON, Japan) was used to observe the surface morphology of the films. XRD analysis was performed with a X′ Pert APD system (Philips, Netherland) using CuKα radiation ($\lambda = 1.54$). The FTIR spectra were obtained by Research Iseries Mattson, U.K.) with 4 cm^{-1} resolution. Film thickness was determined by Alpha-Step 500 (KLA-Tencor, U.S.A.). SPM (ThermoMicroscops, U.S.A.) with a contact AFM mode was used to measure the surface roughness and observe the surface topography of the films. TGA/DTA study was made with SDT2960 (TA instruments, U.S.A.).

3. Results and Discussion

Figure 2 shows SEM photographs of the surfaces and the cross-sections of as-deposited CN films onto a silicon substrate with 30% nitrogen incorporation. The RF power was 300 W, the DC bias was −80 V, the deposition time was 20 min, and the heating temperature was 150°C, respectively. As shown in Fig. 2(a), the deposited film has small grains with a hexagonal structure. The grain size of the carbon nitride film on the Si substrate is too small; the film deposited on Al_2O_3 (Fig. 2(c)), however, shows crystalline structures clearly. The cross-section of the film (Fig. 2(b)) shows a clear border between CN film and Si-wafer. Then, the thickness of deposited film was about 346 nm.

Figure 3 shows the relationship between thickness and nitrogen incorporations in the range of 0 to 100% with different deposition times. The film thickness increases with the nitrogen gas (%) content in all three cases. Addition of argon in the sputtering gas mixture should enhance the sputtering rate of graphite from the target, because the sputtering yield of graphite by Ar gas is expected to be higher due to higher mass. In this case, it is expected that the deposition rate would decrease with increase in nitrogen gas content in the Ar/N_2 gas mixture. The deposition rate monotonically increases with nitrogen gas content(%) in Fig. 3. This increase is probably due to substrate effect rather than

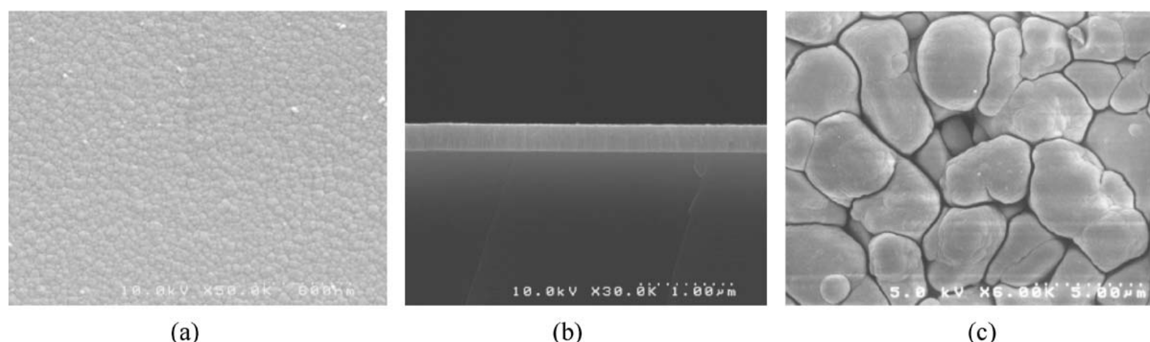

Fig. 2. SEM photographs of CN films: (a) surface of film deposited on Si-wafer, (b) cross section of film deposited on Si-wafer and (c) surface of film deposited on Al_2O_3 substrate.

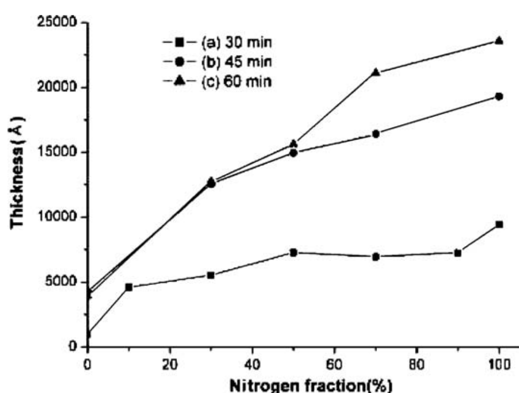

Fig. 3. The thickness of CN films as a function of nitrogen gas (%) on Si_3N_4 substrate, keeping substrate negative bias at 80 V and working pressure at 1×10^{-2}.

the sputtering effect at the target by Ar. Both energetic and neutral Ar species probably enhance the nitrogen species' mobility and increase N sticking at the growth surface. This also supports the previous report that Ar acts as a nitrogen carrier, which, in turn, enhances the deposition rate [15].

Figure 4 shows the XRD spectra of the as-deposited carbon nitride films on the Si-wafer with the different DC biases. Several experimental data registered in ICDD (International Center for Diffraction Data) were used for reference (50-0845, 50-1249, 50-1250, 50-1512) [16–18]. All samples in Fig. 4 show β-C_3N_4(200) and lonsdaleite(102) peaks, i.e. 32.533° (PDF 50-1512) and 61.852° (PDF 19-0268), respectively. The strong peak at 69.19° is the Si (400) peak with d-spacing, 1.3569 A. There are no graphite peaks in the films. These results reveal that the complete chemical reaction was occurred during the film formation. As shown in Fig. 4, as the absolute value of the DC bias increases from −30 to −90 V, the β-C_3N_4 (200) peak intensity increases. However, we did not observe a considerable change in the lonsdaleite (102) peak intensity according to DC bias.

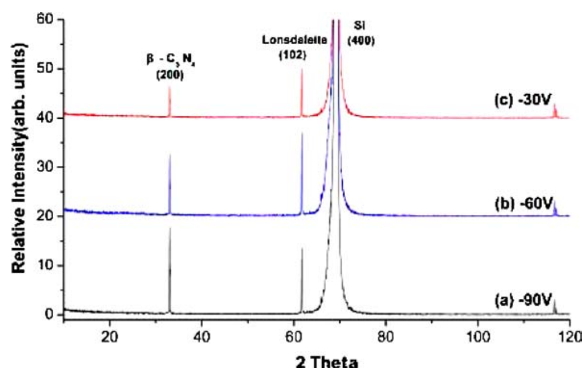

Fig. 4. XRD patterns of CN film on Si-wafer with diferent DC bias.

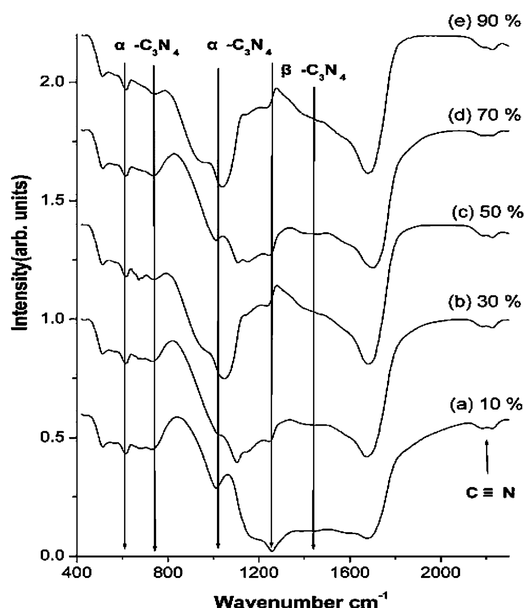

Fig. 5. FTIR spectrum of CN films on Si_3N_4 substrate with various nitrogen gas (%). RF power is 300 W, the DC bias is −80 V, the deposition time is 20 min and the heating temperature is 150°C, respectively.

To understand the bonding state of the films, we performed the FTIR analysis. The calculated data by Zhang et al. [19] was referred to verify the presence of crystalline carbon nitride, e.g. α-C_3N_4, β-C_3N_4. Figure 5 shows the FTIR spectra of five samples with different nitrogen ratios. The peaks at 606, 753, 1011 and 1257 cm^{-1} are attributed to α-C_3N_4 absorption bands. The weak peak at 1448 cm^{-1} is β-C_3N_4 absorption band. Due to the C≡N stretching mode, the weak peak is observed at 2200 cm^{-1}. The band between 1500 and 1800 cm^{-1} is due to the sp^2 carbon atoms bonded to nitrogen atoms, a bond which form the main network of the material [20]. Figure 5 shows only small differences between the spectra of the samples deposited with different nitrogen ratios.

The roughness study in which the samples were heated was performed with averaging by 5 point random scanning in 2 μm × 2 μm area. Figure 6 shows 3-D AFM images of the film deposited on the Si_3N_4 substrate with 1 hr deposition time: N_2 ratio is 70%, RF

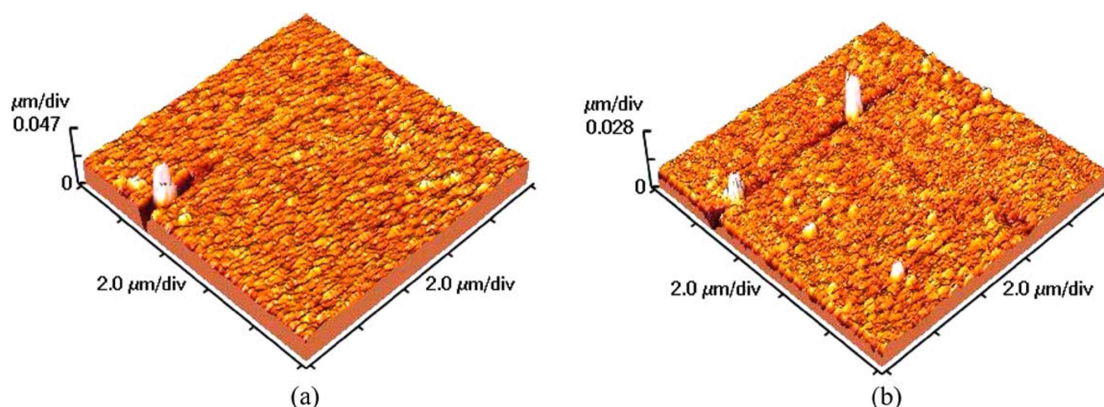

Fig. 6. AFM images of CN films prepared at 300 W, 1 hour, in non-heated chamber (a) and in heated chamber (b) at 150°C.

power is 300 W, negative DC bias is 40 V, and the distance between the substrate and target is 5 cm. The average rms roughness in Fig. 6(a) (b) are 1.2188 nm and 1.4638 nm, respectively. We can find that the deposited film surface was composed of very fine grain from the topography of Fig. 6. The film roughness and grain size of the heated sample at 150°C are larger than those of the non-heated sample. The sputtering yield can be accelerated. The substrate etching occurred simultaneously by the extra thermal energy supplied from the heating source. Therefore, the deposition rate and films roughness increased.

Figure 7 shows the thermal stability of as-deposited CN films at 300 W RF power. Heating temperature was raised from room temperature to 1400°C at a heating rate of 10°C/min, in pure nitrogen atmosphere, and with

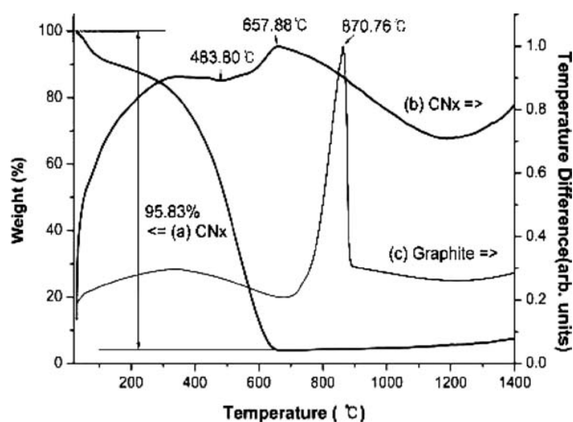

Fig. 7. TGA/DTA curves of as-deposited CN films and graphite powder; TGA for CN film (a), DTA for CN film (b) and graphite powder (c).

Al_2O_3 reference. There were neither exothermic nor endothermic peaks, implying the absence of any phase transition when the processing temperature exceeded 650°C at the TGA and 658°C at the DTA, respectively. Furthermore, as can be seen from the TGA curve between 650°C and 1400°C tends to be flat, implying some kind of stable C—N bonding in this film. This result indicates that our film had a very stable phase in thermodynamics below 1400°C equipment limited temperature. At temperature above 650°C, the weight of the film increases slightly. A similar result was reported by X.C. Xiao et al. [12]. They suggested that some kind of phase transition of carbon nitride occurrs in this temperature region. At the temperature around 600°C, the TGA curve drops rapidly. This drop occurs because the chain of the weakly bonded C—N is broken and some carbon species are thermally desorbed. Figure 7(c) shows DTA curve of the graphite target powder. This is different from Fig. 7(b) which is the curve of CN films.

Figure 8 shows the XPS spectrum of C 1s and N 1s electrons of CN films as a function of nitrogen ratio($N_2/(N_2 + Ar)$). According to the nitrogen gas ratio, the C 1s peaks are shifted to the right about 2 eV from the β-C_3N_4 peak, 286.2 eV [22] and 286.8 eV [23]. However, the N 1s peaks are very close to β-C_3N_4 peaks, 398.6 eV [24] and 398.6 eV [25]. It can be considered that the deposited films are rich in C—C bond but the theoretical β-C_3N_4 film is not. Atomic concentrations of C and N can be calculated from the XPS data. When the nitrogen ratios are 30, 50 and 70%, the nitrogen incorporations are 34.3, 31.4 and 32.7%, respectively. It can be suggested that the film has a partial β-C_3N_4 phase but not a complete one.

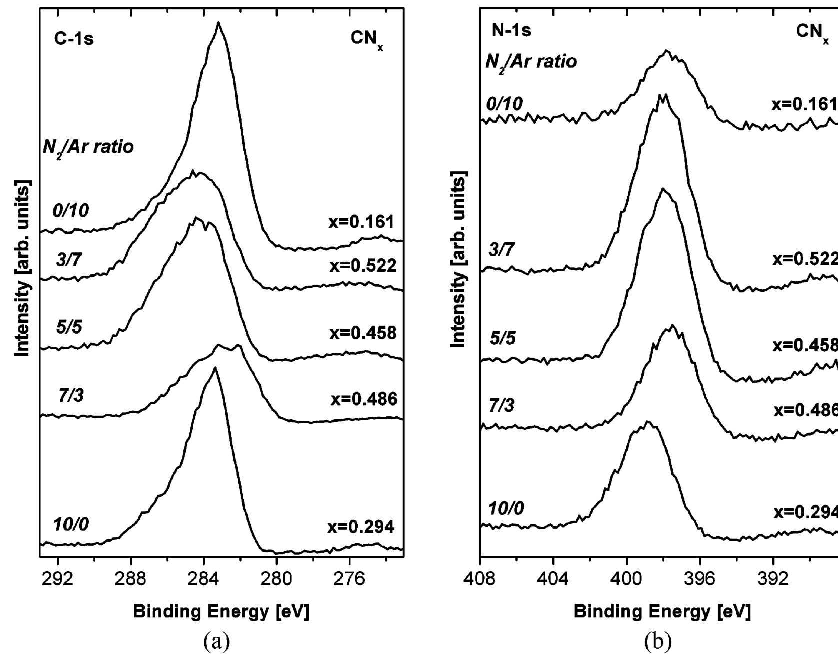

Fig. 8. The X-ray photoelectron spectrum of C 1s (a) and N 1s (b) electrons of CN films.

4. Conclusions

The carbon nitride films with α-C_3N_4, β-C_3N_4 and lonsdaleite have been synthesized by reactive magnetron sputtering with negative DC bias. XRD results showed that the films possessed β-C_3N_4 structure with 32.533°, and FTIR study also showed β-C_3N_4 (1448 cm^{-1}) and α-C_3N_4(606, 753, 1011 and 1257 cm^{-1}) peaks. β-C_3N_4 peak increased with increasing negative DC bias from -30 V to -90 V. The film thickness increased with increasing the nitrogen ratio. The film growth rate deposited on Si_3N_4 substrate with 70% nitrogen ratio and 1 hr deposition time was about 2.2 μm/hr. The film possessed smooth surface morphology about 1.2188 nm (non-heated chamber). It showed no weight loss and phase transition between 650°C and 1400°C. The deposited films consisted of a complex CN_x compound of two crystalline phases: β-C_3N_4 and α-C_3N_4. They also possessed high thermal stability and smooth surface morphology.

Acknowledgment

The authors wish to acknowledge the financial support of Kyungnam University made in the program year of 2003.

References

1. M.L. Cohen, *Phys. Rev.*, B **32**, 7988 (1985).
2. A.Y. Liu and M.L. Cohen, *Science*, **245**, 841 (1989).
3. A.Y. Liu and M.L. Cohen, in *Atomic scale Calculations of Structure in Materials*, edited by M.A. Schluter and M.S. Daw (Materials Research Society, Pittsburgh, 1990).
4. A.Y. Liu and M.L. Cohen, *Phys. Rev.*, B **41**, 10727 (1990).
5. J.L. Corkill and M.L. Cohen, *Physical Review*, B **48**, 17622 (1993).
6. K.M. Yu, M.L. Cohen, E.E. Haller, W.L. Hansen, A.Y. Liu, and I.C. Wu, *Phys. Rev.*, B **49**, 5034 (1994).
7. S.P. Lee and J.B. Kang, *Microchemical Journal*, **70**, 239 (2001).
8. H. Han and B.J. Feldman, *Solid State Commun.*, **65**, 921 (1988).
9. D.W. Wu, W. Fan, H.X. Guo, M.B. He, X.Q. Meng, and X.J. Fan, *Solid State Commun.*, **103**, 193 (1997).
10. P. Gonzalez, R. Soto, E.G. Parada, X. Redondas, S. Chiussi, J. Serra, J. Pou, B. Leon, and M. Perez-Amor, *Appl. Surf. Sci.*, **109–110**, 380 (1997).
11. C.W. Ong, X.-A. Zhao, Y.C. Tsang, C.L. Choy, and P.W. Chan, *Thin Solid Films*, **280**, 1 (1996).
12. K.J. Boyd, D. Marton, S.S. Todorov, A.H. Al-Bayati, J. Kulik, R.A. Zuhr, and J. W. Rabalais, *J. Vac. Sci. Technol.*, A **13**, 2110 (1995).
13. C.M. Sung and M. Sung, *Materials Chemistry and Physics*, **43**, 1 (1996).
14. D.M. Teter and R.J. Hernley, *Science*, **271**, 56 (1996).
15. W. Zheng, T. Ding, I. Ivanov, and J.-E. Sundgren, J. *Mater. Sci. Technol.*, **13**, 154 (1997).

16. R.C. DeVries, Mater. *Res. Innovations*, **1**, 161 (1997).
17. Y.A. Li, S. Su, H.S. Li, and W.Y. Luo, *J. Mater. Sci. Lett.*, **17**, 31 (1998).
18. J.P. Riviere, D. Texier, J. Delafond, M. Jaonen, E.L. Mathe, and J. Chanmont, *Materials Letters*, **22**, 115 (1995).
19. Y. Zhang and Y. Gu, *Philosophical Magazine Letters*, **81**, 505 (2001).
20. C. Popov, M.F. Plass, R. Kassing, and W. Kulisch, *Thin Solid Films*, **333**, 406 (1999).
21. X.C. Xiao, Y.W. Li, W.H. Jiang, L.X. Song, and X.F. Hu, *J. Phys. Chem. Solids*, **61**, 915 (2000).
22. C. Jama, V. Rousseau, O. Dessaux, and P. Goudmand, *Thin Solid Films*, **302**, 58 (1997).
23. R. Alexandrescu, F. Huisken, A. Crunteanu, S. Petcu, S. Cojocaru, S. Cireasa, and I. Morjan, *Appl. Phys. A*, **65**, 207 (1997).
24. M. Kohzaki, A. Matsumuro, T. Hayashi, M. Muramatsu, K. Yamaguch, *Thin Solid Films*, **308/309**, 239 (1997).
25. H.W. song, F.Z. Cui, X.M. He, W.Z. Li, and H.D. Li, *J. Phys. Conden. Matt.*, **6**, 6125 (1994).